Unconventional Transport in the "Hole" Regime of a Si Double Quantum Dot

Teck Seng Koh, C. B. Simmons, M. A. Eriksson, S. N. Coppersmith, and Mark Friesen
Department of Physics, University of Wisconsin-Madison, Madison, Wisconsin 53706, USA
(Received 1 September 2010; published 4 May 2011)

Studies of electronic charge transport through semiconductor double quantum dots rely on a conventional "hole" model of transport in the three-electron regime. We show that experimental measurements of charge transport through a Si double quantum dot in this regime cannot be fully explained using the conventional picture. Using a Hartree-Fock (HF) formalism and relevant HF energy parameters extracted from transport data in the multiple-electron regime, we identify a novel spin-flip cotunneling process that lifts a singlet blockade.

DOI: 10.1103/PhysRevLett.106.186801 PACS numbers: 73.63.Kv, 73.21.La, 73.23.Hk, 85.35.Be

In quantum computing, semiconductor quantum dots have long been considered as good candidates for qubits [1–3]. A promising architecture for such qubits is the double quantum dot [3–5]. Understanding spin-dependent transport [6–10] is important for using the spin degree of freedom in a double dot qubit. Here, we show that transport data taken in the three-electron regime of a double dot in a Si/SiGe heterostructure have features that are qualitatively inconsistent with the conventional model of "hole" transport [11], because this model does not account for transport through excited states. Using the Hartree-Fock (HF) formalism with singly excited configurations [12], together with relevant HF parameters extracted from the transport data (see [13]), we demonstrate that the striking features in the data arise from a novel spin-flip cotunneling process in which the multielectron nature of the system enters fundamentally.

Several experiments have probed charge transport through double quantum dots in the few-electron regime and investigated effects such as energy-dependent tunneling and spin-dependent transport [6–10]. Transport in the three-electron regime is well described in terms of holes when all the intradot relaxation rates are much faster than the interdot tunnel rate, so that the dominant transport channels are through the lowest energy states of each dot, as is typically the case in GaAs devices [9,11].

Our theoretical work is based on data [8], in which a lateral double quantum dot was formed by electrostatic gating of a Si/SiGe heterostructure, as shown in the inset of Fig. 1(a). Figure 1(a) shows source-drain current versus controlling gate voltages at a fixed source-drain bias voltage. Transport through the two dots is energetically favorable within triangular regions whose size is determined by the source-drain bias. Lines of high current in these bias triangles are associated with fast tunneling between the dots and between the dots and the leads [11]. From the orientation of the line $\alpha\beta$ in Fig. 1(b), we deduce that it is associated with the resonance of an energy level in the "left" dot with the chemical potential in the left lead. Quantitative fits allow the edges of the triangles to be determined and are reported in detail in Ref. [13]. Figure 1(b) is a schematic diagram of the bias triangles, with energy axes shown in the inset. The lower features arise from transport when the double dot contains either one or two electrons ("two-electron" regime), while the upper features reflect transport when the dot contains either two or three electrons ("three-electron" regime, also conventionally termed the "hole" regime).

There are two regions of current flow in each transport regime, shown in Fig. 1(a). Each of these regions of current is contained in a triangle, shown in either blue or red in Fig. 1(b). The presence of current in the blue triangle implies that there is significant transport through excited states of the dots [8,13], something that has recently been observed in transport through a single phosphorous donor in silicon as well [14].

Because the effective electronic mass in Si is much larger than in GaAs, transport is energetically favorable within each bias triangle, but the triangle is not entirely filled because the electron tunneling rate is strongly energy-dependent [6–8]. The two parallel lines of high current that are observed along the left edges of the singlet and triplet triangles in the two-electron regime (lower feature) indicate that energy-dependent tunneling across the left barrier is the bottleneck in the total tunneling rate [13].

In the three-electron regime, the conventional picture that describes the conduction in terms of holes predicts that there should be two parallel lines of high current [Fig. 1(c)]. This is because, in the two-electron regime, electron occupancy cycles through the states $(1, 0) \rightarrow (2, 0) \rightarrow (1, 1)$, and the three-electron regime is modeled conventionally [11] as hole transport in the opposite direction: $(1, 1) \rightarrow (0, 2) \rightarrow (0, 1)$, where the numbers represent electron or hole occupancy in the left and right dots. Because of particle-hole symmetry, the hole picture predicts parallel lines of high current similar to the data in the two-electron regime [Fig. 1(c)].

The transport data in Fig. 1(a) are inconsistent with a picture in terms of holes, as it shows two lines of high

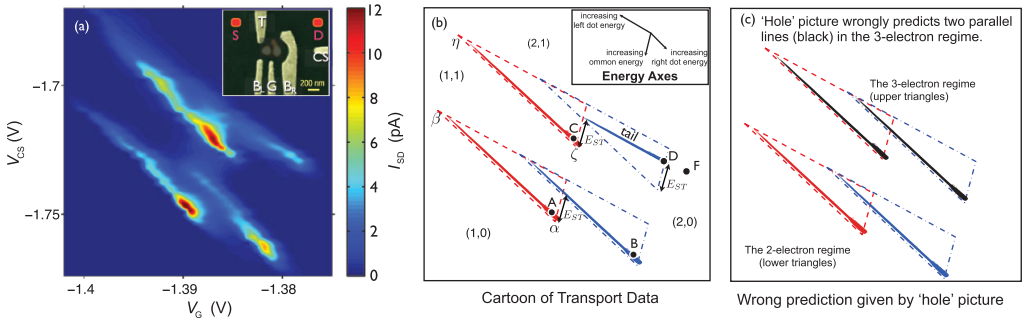

FIG. 1 (color). (a) Transport current I_{SD} in a Si/SiGe double quantum dot (color scale) as a function of controlling gate voltages, V_G (V) and V_{CS} (V), reported in Ref. [8]. Inset shows an SEM image of the gates with a numerically simulated double dot overlayed. White letters (T, B_L, G, B_R and CS) label gates and red letters (S, D) label the source and drain. For this data, electrons flow from left to right. (b) A cartoon of the bias triangles and lines of high current. Inset shows the energy axes of the dots. The lower (upper) features are the electron (hole) triangles. Red dashed lines represent current through the singlet (singletlike) channel of the electron (hole) bias triangle and blue dot-dashed lines the triplet (tripletlike) triangle. A and B are resonant peaks of the singlet and triplet electron triangles. C is the resonant peak of the singletlike hole triangle. A and C are the triple points at the boundary of the (1,0), (1,1), (2,0) and (1,1), (2,0), (2,1) charge occupations. F lies along the line extending from the tail; it is a representative point where cotunneling is dominant. E_{ST} is the (2,0) singlet-triplet energy splitting. Data are obtained at a reverse-bias source-drain voltage, $V_{SD} = -0.274$ mV, first published in Ref. [8] as -0.3 mV. Ref. [13] details the quantitative fits to identify the triangles. (c) The prediction using the conventional hole picture in the three-electron regime is shown as two parallel lines (black), which is inconsistent with the tail observed in the data.

current in the three-electron regime (upper feature) that are clearly not parallel. In this regime, there is a line of high current at the left edge of the bias triangle (line $\zeta\eta$) for ground state transport, which is expected since the left barrier is observed to be the bottleneck in the two-electron regime. However, in the bias triangle for excited state transport, there is a ''tail'' parallel to the right edge but away from it, which the hole picture completely fails to describe.

To understand the problem theoretically, we formulate it in terms of chemical potentials and use the Hartree-Fock (HF) approximation with singly excited configurations to determine the spin eigenfunctions and energy levels of each of the double dot states involved in the three-electron regime. The relevant parameters in the HF formulation are extracted from the transport data as detailed in Ref. [13]. From the energy levels and possible transitions between states, we calculate the electrochemical potentials for charging or discharging a dot by one electron [15]. The four relevant electrochemical potentials for the dots are shown for the two-electron case in Figs. 2(a) and 2(b). For the three-electron case, the full set of ten electrochemical potentials, shown in Figs. 2(c) and 2(d), is clearly greater than the four electrochemical potentials for transport modeled on two holes. The many-electron nature of the problem thus enters our analysis of transport naturally.

Without going into the details of the HF calculations, we can gain some insight into the possible (2, 1) states using qualitative arguments. The pure singlet and triplet states, $S(2,0)$ and $T(2,0)$, are no longer orthogonal when we include a weak coupling to a third electron in the right dot. The perturbation leads to a ''singletlike'' ground state $S^*(2,1)$, whose spin configuration in the left dot is mainly $S(2,0)$ with a small admixture of $T(2,0)$. The $S^*(2,1)$ state has spin $S_z = \pm 1/2$ and is doubly degenerate. The perturbation also leads to ''tripletlike'' states $T^*(2,1)$, for which spin addition gives $S_z = \pm 1/2$ or $\pm 3/2$. The $S_z = \pm 1/2$ states contain mainly triplet $T(2,0)$ with a small admixture of $S(2,0)$. The $S_z = \pm 3/2$ states have spins that are either all up or all down; they are doubly degenerate without any admixture of singlet states. The triplet degeneracies are lifted due to the fact that exchange energies are different for different three-electron spin configurations. The energy splittings arise from interdot interactions, which are much smaller than intradot interactions. Thus, the splittings within the tripletlike manifold are much finer than the splitting between the singletlike and tripletlike manifolds. These arguments are borne out by our calculations [15].

From the energy levels calculated with the HF Hamiltonian, we can explain how the electrochemical potentials, shown in Fig. 2(c), are obtained. In the three-electron regime, electron occupancy cycles through $(1,1) \rightarrow (2,1) \rightarrow (2,0)$. The first transition corresponds to charging of the left dot from a (1, 1) to a (2, 1) state. For clarity, we do not distinguish between the two closely spaced (1, 1) energies, nor do we distinguish between the three closely spaced $T^*(2,1)$ energies. We therefore obtain two distinct electrochemical potentials, μ_{c,T^*} and μ_{c,S^*}, shown in Fig. 2(c), which are the energies needed to charge the left dot from a (1, 1) state to the $T^*(2,1)$ and $S^*(2,1)$ states, respectively. The second transition represents the discharge of an electron from a (2, 1) to a (2, 0) state. Electrochemical potentials, μ_{d,T^*} and μ_{d,S^*}, drawn on the right dot, represent the discharge of the right dot from $T^*(2,1)$ to $T(2,0)$ and $S^*(2,1)$ to $S(2,0)$ respectively.

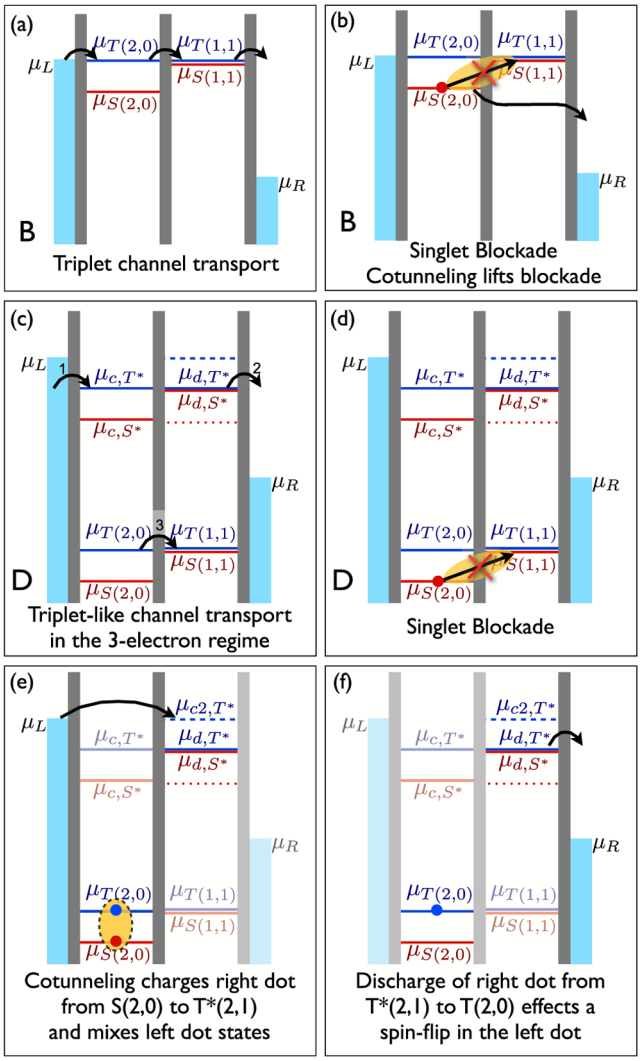

FIG. 2 (color online). Diagrams for transport through excited states and the process of spin-flip cotunneling. (a) Triplet channel transport in the two-electron regime. At B, the resonant peak of the triplet channel, transport is allowed through the triplet levels, $\mu_{T(2,0)}$ and $\mu_{T(1,1)}$. (b) When the singlet level $\mu_{S(2,0)}$ is loaded, transport is energetically uphill and blockaded. Cotunneling of a left dot electron out to the right lead lifts the blockade to resume triplet channel transport. (c) In the three-electron regime, transport occurs in the following cycle: step 1, $(1,1) \rightarrow (2,1)$; step 2, $(2,1) \rightarrow (2,0)$; step 3, $(2,0) \rightarrow (1,1)$. At D, these occur through the tripletlike channel (blue). (d) Because of the loading of the singletlike μ_{c,S^*} level (red) at D, the system ends up in the $S(2,0)$ state, whereby transport is blockaded. (e) When an electron cotunnels from the left lead into the right dot to form a tripletlike state, it puts the left dot into an admixture of singlet and triplet. (f) The right dot discharges from μ_{d,T^*}, leaving a triplet state in the left dot, thus causing a spin-flip and resuming transport.

These are the continuous lines (blue and red) on the right dot in Fig. 2(c). Because of singlet-triplet mixing in the left dot, two other transitions of much smaller likelihood are possible. They are the $S^*(2,1)$ to $T(2,0)$ and $T^*(2,1)$ to $S(2,0)$ transitions, represented by the red dotted and blue dashed levels, respectively, in the same figures. The last step in the cycle is the interdot transition, $(2,0) \rightarrow (1,1)$. The chemical potentials in this step are identical to the two-electron case [Figs. 2(a) and 2(b)] and are labeled as $\mu_{S,T(2,0)}$ and $\mu_{S,T(1,1)}$.

We can now explain the tail in the transport data, which, as described above, is a prominent feature that is qualitatively inconsistent with a description in terms of holes. At point D in Fig. 2(c), transport is allowed through the blue tripletlike levels. However, it is also possible to load the red singletlike μ_{c,S^*} level. In this case, as the right dot discharges, the system is likely to end up in the $S(2,0)$ state, where transport is energetically uphill and therefore blockaded [Fig. 2(d)]. We call this a "singlet blockade." The lifting of the singlet blockade along the tail is shown in sequence in Figs. 2(e) and 2(f). Starting from $S(2,0)$, the double dot forms a tripletlike $T^*(2,1)$ state when an electron from the left lead cotunnels into the right dot, as shown in Fig. 2(e). The charging of the right dot in this transition requires the same energy as its reverse discharging process ($T^*(2,1)$ to $S(2,0)$), represented by the blue dashed line in Fig. 2(c). It is labeled by μ_{c2,T^*} in Figs. 2(e) and 2(f). Because the tripletlike state contains an admixture of singlet and triplet states in the left dot, when the right dot discharges from the μ_{d,T^*} level, the left dot ends up in the triplet (2,0) state, thus causing a spin-flip. With the singlet blockade lifted, the system then completes the cycle into the triplet (1,1) state and transport resumes as shown in Fig. 2(c). We term this process "spin-flip cotunneling."

The tail in the transport data in Fig. 1(a) is bright along its entire length because the chemical potentials for the right dot and the left lead are the same. Point D is the brightest point along the tail because of the fast interdot tunneling when $\mu_{T(2,0)}$ is aligned with $\mu_{T(1,1)}$.

The spacing of the tail away from the edge of the triangle is consistent with the energy difference between the μ_{c2,T^*} and μ_{d,T^*} levels on the right dot [Fig. 2(e)] being equal to E_{ST}, the (2,0) singlet-triplet energy splitting. To understand how this is consistent with the transport data, we start from point C in Fig. 1(b) and note that when both dot energies fall by E_{ST}, the blue, dashed μ_{c2,T^*} level of the right dot lines up with the Fermi level of the left lead. This measure of E_{ST} is also consistent with other measures of ST splitting [13].

The significant role cotunneling plays in the triplet and tripletlike transport channels of the two and three-electron regime is interesting. In both cases, cotunneling by itself does not contribute significantly to the current, but plays the role of allowing transport to resume by lifting the singlet blockade.

Current will flow through the tripletlike channel when the loading rate is comparable to the unloading rate in the singletlike channel [15]. In the Supplementary Information, we estimate these rates and find that they are

indeed the same order of magnitude. The blockade is therefore lifted about as quickly as it is encountered. In this way, spin-flip cotunneling enables transport through the tripletlike channel. The resulting current is that of the unblockaded, tripletlike channel, reduced by a factor of ~2 [15].

Interestingly, transport via the triplet channel was not observed in the experiments reported in Ref. [9]. In that study, a conventional hole model was sufficient to describe transport in the three-electron regime, as consistent with the fact that transport occurred through the ground states in the two-electron regime.

It is also interesting to compare the intradot spin-flip times with interdot tunneling times for GaAs and Si. In GaAs devices, spin-flip times range from ~200 μs for a two-electron dot [16], to ~0.85 ms (at 8 T [17]) and >1 s (at 1 T and 120 mK [18]) for single electron dots. Recent experiments report spin-flip times in single electron dots in Si [19–22] ranging from 40 ms (at 2 T [19]) to 6 s (at 1 T [20]), at low temperatures. The tunnel coupling for the same Si double dot studied here was found to be 10 ns (25 ns) in the elastic (inelastic) tunneling regime [13]. However, tunnel couplings for electrostatically gated semiconductor double dots are tunable and can be both larger or smaller than spin-flip times.

Finally, note that a pulsed gate experiment is proposed in [15], which would allow us to probe singletlike and tripletlike states more directly.

In summary, we have shown that the conventional hole model of transport in the three-electron regime fails qualitatively because of the importance of excited state transport. The Hartree-Fock formalism, with relevant parameters fitted to transport data, leads to the description of a model which explains all of the features of the transport data, including a novel process of spin-flip cotunneling.

We thank Nakul Shaji for useful discussions and gratefully acknowledge funding from ARO and LPS (W911NF-08-1-0482) and NSF (DMR-0805045).

[1] Daniel Loss and David P. DiVincenzo, Phys. Rev. A **57**, 120 (1998).
[2] D. P. DiVincenzo, D. Bacon, J. Kempe, G. Burkard, and K. B. Whaley, Nature (London) **408**, 339 (2000).
[3] J. M. Taylor, H.-A. Engel, W. Dür, A. Yacoby, C. M. Marcus, P. Zoller, and M. D. Lukin, Nature Phys. **1**, 177 (2005).
[4] Jeremy Levy, Phys. Rev. Lett. **89**, 147902 (2002).
[5] J. R. Petta, A. C. Johnson, J. M. Taylor, E. A. Laird, A. Yacoby, M. D. Lukin, C. M. Marcus, M. P. Hanson, and A. C. Gossard, Science **309**, 2180 (2005).
[6] K. Ono, D. G. Austing, Y. Tokura, and S. Tarucha, Science **297**, 1313 (2002).
[7] J. R. Petta, A. C. Johnson, A. Yacoby, C. M. Marcus, M. P. Hanson, and A. C. Gossard, Phys. Rev. B **72**, 161301 (2005).
[8] Nakul Shaji, C. B. Simmons, Madhu Thalakulam, Levente J. Klein, Hua Qin, H. Luo, D. E. Savage, M. G. Lagally, A. J. Rimberg, R. Joynt, M. Friesen, R. H. Blick, S. N. Coppersmith, and M. A. Eriksson, Nature Phys. **4**, 540 (2008).
[9] A. C. Johnson, J. R. Petta, C. M. Marcus, M. P. Hanson, and A. C. Gossard, Phys. Rev. B **72**, 165308 (2005).
[10] H. W. Liu, T. Fujisawa, Y. Ono, H. Inokawa, A. Fujiwara, K. Takashina, and Y. Hirayama, Phys. Rev. B **77**, 073310 (2008).
[11] W. G. van der Wiel, S. De Franceschi, J. M. Elzerman, T. Fujisawa, S. Tarucha, and L. P. Kouwenhoven, Rev. Mod. Phys. **75**, 1 (2002).
[12] A. Szabo and N. Ostlund, *Modern Quantum Chemistry* (Dover, New York, 1996).
[13] C. B. Simmons, Teck Seng Koh, Nakul Shaji, Madhu Thalakulam, L. J. Klein, Hua Qin, H. Luo, D. E. Savage, M. G. Lagally, A. J. Rimberg, Robert Joynt, Robert Blick, Mark Friesen, S. N. Coppersmith, and M. A. Eriksson, Phys. Rev. B **82**, 245312 (2010).
[14] G. P. Lansbergen, R. Rahman, J. Verduijn, G. C. Tettamanzi, N. Collaert, S. Biesemans, G. Klimeck, L. C. L. Hollenberg, and S. Rogge, arXiv:1008.1381v1.
[15] See supplemental material at http://link.aps.org/supplemental/10.1103/PhysRevLett.106.186801 for details of our calculations.
[16] Toshimasa Fujisawa, David Guy Austing, Yasuhiro Tokura, Yoshiro Hirayama, and Seigo Tarucha, Nature (London) **419**, 278 (2002).
[17] J. M. Elzerman, R. Hanson, L. H. Willems van Beveren, B. Witkamp, L. M. K. Vandersypen, and L. P. Kouwenhoven, Nature (London) **430**, 431 (2004).
[18] S. Amasha, K. MacLean, Iuliana P. Radu, D. M. Zumbühl, M. A. Kastner, M. P. Hanson, and A. C. Gossard, Phys. Rev. Lett. **100**, 046803 (2008).
[19] M. Xiao, M. G. House, and H. W. Jiang, Phys. Rev. Lett. **104**, 096801 (2010).
[20] Andrea Morello, Jarryd J. Pla, Floris A. Zwanenburg, Kok W. Chan, Kuan Y. Tan, Hans Huebl, Mikko Möttönen, Christopher D. Nugroho, Changyi Yang, Jessica A. van Donkelaar, Andrew D. C. Alves, David N. Jamieson, Christopher C. Escott, Lloyd C. L. Hollenberg, Robert G. Clark, and Andrew S. Dzurak, Nature (London) **467**, 687 (2010).
[21] Robert R. Hayes, Andrey A. Kiselev, Matthew G. Borselli, Steven S. Bui, Edward T. Croke III, Peter W. Deelman, Brett M. Maune, Ivan Milosavljevic, Jeong-Sun Moon, Richard S. Ross, Adele E. Schmitz, Mark F. Gyure, and Andrew T. Hunter, arXiv:0908.0173v1.
[22] C. B. Simmons, J. R. Prance, B. J. Van Bael, Teck Seng Koh, Zhan Shi, D. E. Savage, M. G. Lagally, R. Joynt, Mark Friesen, S. N. Coppersmith, and M. A. Eriksson, Phys. Rev. Lett. **106**, 156804 (2011).